Hindawi
Journal of Chemistry
Volume 2019, Article ID 5675870, 9 pages
https://doi.org/10.1155/2019/5675870

*Research Article*

# A Computational and Structural Database Study of the Metal-Carbene Bond in Groups IA, IIA, and IIIA Imidazol-2-Ylidene Complexes

**Samuel Tetteh**

*Department of Chemistry, School of Physical Sciences, College of Agriculture and Natural Sciences, University of Cape Coast, Cape Coast, Ghana*

Correspondence should be addressed to Samuel Tetteh; stoshgh2001@yahoo.com

Received 27 October 2019; Revised 30 November 2019; Accepted 11 December 2019; Published 24 December 2019

Academic Editor: Robert Zaleśny



Imidazol-2-ylidenes are important N-heterocyclic carbenes which have become universal ligands in organometallic and coordination chemistry. Generally classified as $\sigma$-donor ligands, these compounds have been used to stabilize various metal complexes which hitherto were less stable in their catalytic processes. Herein, the number and distribution of group IA, group IIA, and group IIIA metal-imidazol-2-ylidene complexes retrieved from the Cambridge Structural Database (CSD) are assessed. The data showed that the mean M-$C_{carbene}$ bond length increases with increasing ionic size but is similar across each diagonal. Dominant factors such as Lewis acidity and electrostatic attractions were found to control the bonding modes of the respective ions. Generally, the metal ions show preference for tetrahedral coordination with larger cations forming complexes with higher coordination numbers. For their high number of entries (101), tetrahedrally coordinated boron complexes with various electron withdrawing and electron donating groups were studied computationally at the DFT/B3LYP level of theory. The strength of the B-$C_{carbene}$ bond was found to depend on steric interactions between bulky groups on the borenium atom and substituents on the N-positions of the imidazol-2-ylidene ligand. This observation was further confirmed by estimation of the binding energy, natural charge, and the electron distribution in the B-$C_{carbene}$ bond.

## 1. Introduction

N-heterocyclic carbenes (NHCs) are important ligands used in the synthesis and study of catalytic systems [1–3]. Since the synthesis of the imidazol-2-ylidene (Im) template, **1a** by Öfele and Wanzlick [4–6] in 1968, a plethora of metal complexes bearing Im ligands have been synthesized and proven as better alternatives to the ubiquitous phosphine metal complexes [7].

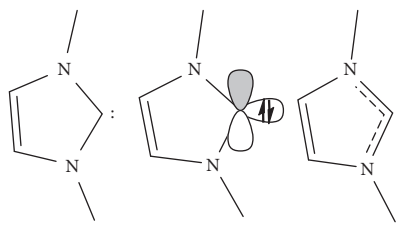


1a 2a 3a

These Im complexes are more stable in processes such as cyclometalation that lead to the degradation of metal phosphine catalysts [8]. They are also employed as key catalysts in the C-C coupling of aromatic aldehydes and related hydroformylation reactions [5, 9, 10]. As reported by Teyssot et al. [11], in vivo studies of NHC complexes of group IB metals investigated for their anticancer properties showed cytotoxicities higher than the reference compound (cisplatin). This relatively better activity can be attributed to the stability of the drug in biological medium before reaching its target site to perform its pharmacological function [12].

Studies on the electronic structure of metal-NHC complexes have shown that NHCs are predominantly $\sigma$-donor ligands with insignificant $\pi$-acceptor properties [7]. According to Jacobsen et al. [7], the carbene carbon is $sp^2$-hybridized with an empty p-orbital orthogonal to the $sp^2$

plane, which gives rise to a singlet $^1A_1$ ($\sigma^2$) ground state as shown in structure **2a**. The two carbene electrons are then available for sigma bonding with a metal atom or ion. The imidazole ring is largely stabilized by donation of p$\pi$-electrons from the N-atoms into the empty orthogonal p-orbitals on the carbene carbon [5] and not by acceptance of $\pi$-electrons from coordinating metal species. The high stability of NHC complexes of main-group and inner-transition elements shows their $\sigma$-donor character [13] since these metals have insignificant backbonding characteristics. A computational and structural database study by Baba et al. [14] has also shown that the carbene carbon can undergo sp-hybridization, **3a**, with substantial s-character to cause metal-carbon bond shortening in NHC-metal complexes.

The metal-carbene bond in main-group metal carbenes is essentially ionic with M-$C_{carbene}$ contacts usually greater than the sum of the van der Waals radii [15]. For a series of group 1 carbenes, the M-C bond strength was found to decrease with increasing atomic number as a result of the reduced Lewis acidity of the $M^+$ ion [16]. The strong acidity of beryllium is an important factor in the stability of Be-NHC complexes. According to Hermann [5], carbene ligands can split the polymeric structure of beryllium dichloride to form tris-carbenic ionic complexes. NBO analysis of the Be-$C_{carbene}$ bond supports a purely $\sigma$-donor interaction since there is no possibility of backbonding in the case of beryllium. The M-L distance is a very important factor in the study of the structure of biomolecules such as proteins (of which the imidazol-2-ylidene is a side chain of the amino acid histidine) [17]. Studies have shown that if $Zn^{2+}$ is replaced with $Cd^{2+}$ in Zn-finger motifs, the requisite conformation is distorted because Cd-bound proteins, though having the same geometry as $Zn^{2+}$, cannot maintain the native conformation because of the increased Cd-N distances relative to the Zn-N distances [18]. The toxicities of $Hg^{2+}$ and $Pb^{2+}$ can also be attributed to the fact that they adopt totally different geometries when bound to proteins. Therefore, understanding the M-L distances and the coordination mode is important for the characterization of different metal ions in different environments [19].

Because of the importance of imidazol-2-ylidenes in stabilizing metal complexes, this work investigates the M-Im distances and coordination geometries of GP IA, IIA, and IIIA complexes bearing at least one imidazol-2-ylidene ligand in the Cambridge Structural Database (CSD). The variation of the bond length down a group, across a given period as well as along a given diagonal, is also assessed. The effect of substituents (electron withdrawing and electron donating) on the B-$C_{carbene}$ bond in tetrahedrally coordinated boranes is also investigated computationally by density functional theory (DFT) methods.

## 2. Methods

*2.1. CSD Analyses.* The Cambridge Structural Database (CSD) program version 5.40 (November 2018) + 1 update and *ConQuest* [20] version 2.1.0 were used for the substructure searches of the main-group metal-imidazol-2-ylidene complexes. The geometry around each metal ion was defined by restricting the number of bonded atoms in each search. The search was further refined by imposing the following secondary search criteria: 3D coordinated determined; crystallographic $R$ factor ≤0.075; no disorder in the crystal structure; no errors; no polymeric structures; and no powder structures and only organometallic structures (according to standard CSD definitions). The number of hits and the respective coordination numbers are shown in Table 1. The reference codes of geometries with only one hit are also given in parenthesis. The CSD program *Mercury* [21] (version 4.1.0) was used for the structure visualization while the associated Data Analysis Module was used for the statistical analyses of the retrieved data.

*2.2. Computational Details.* All calculations were performed with the Gaussian 09 package [22]. The input and output files were visualized using the GaussView 5.0.8 [23] molecular viewer. The gas phase structures of the boron complexes were fully optimized at the density functional theory (DFT) using Becke's three parameter hybrid method and the Lee–Yang–Parr correlation functional (B3LYP) [24] with the 6–311++G** basis set to include polarization and diffuse functions on all atoms. These were done without symmetry constraints. Vibrational frequency analysis of the optimized structures was performed to ensure that the potential energy of the structures was at a minimum and the molecules were in their ground states [25].

## 3. Results and Discussion

The Cambridge Structural Database (CSD) is a repository of high-resolution X-ray crystal structures with the version 5.40 (November 2018) + 1 update containing over 975000 entries. These are made up of organic and metal organic structures which have been synthesized or extracted and crystallized under various conditions. The stability of these solid-phase structures has been used to discuss and predict the geometry and coordination modes of several metal ions in various ligand environments [17, 18, 26]. The distribution of the metal-ligand bond in various environments has also been studied using data from the CSD [17]. An understanding of the M-L distances and the coordination geometries of metal ions will help to elucidate the mechanism of reaction as well as the geometric function of the respective metal ion in different ligand environments. A total of 431 crystal structures comprising 73 group IA, 45 group IIA, and 313 group IIIA metal-imidazol-2-ylidenes were retrieved from the database.

Table 1 shows the distribution of the M-Im bond distances and the Im-M-X bond angles (where $X$ is any other ligand or anion other than Im) as well as the coordination number and the number of hits of imidazol-2-ylidene coordinated group IA compounds retrieved from the CSD. The reference codes of geometries with only one entry in the database are given in parenthesis.

Lithium NHC complexes have largely been synthesized for their ability to act as transmetalation agents [13]. Li-Im

Table 1: The number of entries (hits), coordination number (CN), and bond parameters of group IA metal-imidazol-2-ylidene complexes.

| Metal | CN | No. of hits | D (M-Im) (Å) | | | Im-M-X angle (°) | |
|---|---|---|---|---|---|---|---|
| | | | Mean | Range | St dev. | Mean | St dev. |
| Li | 2 | 3 | 2.141 | 2.075–2.178 | 0.034 | 170.23 | 12.45 |
| | 3 | 15 | 2.131 | 2.018–2.335 | 0.073 | 123.6 | 13.75 |
| | 4 | 20 | 2.191 | 2.047–2.338 | 0.062 | 111.8 | 18.09 |
| | 5 | 2 | 2.111 | 2.103–2.119 | 0.008 | 106.2 | 19.31 |
| | 6 | 1 (MALRAS) | 2.156 | | | | |
| Na | 2 | 4 | 2.447 | 2.439–2.46 | 0.007 | 169.5 | 3.45 |
| | 3 | 3 | 2.46 | 2.388–2.577 | 0.062 | 124.3 | 39.63 |
| | 4 | 7 | 2.505 | 2.468–2.551 | 0.027 | 119.2 | 7.87 |
| K | 2 | 6 | 2.915 | 2.81–3.199 | 0.158 | 178 | 5.41 |
| | 3 | 2 | 3.008 | 2.989–3.024 | 0.030 | 133.3 | 3.79 |
| | 4 | 4 | 2.928 | 2.901–2.954 | 0.030 | 100.6 | 19.31 |
| | 5 | 3 | 3.054 | 2.921–3.132 | 0.099 | 108.4 | 32.67 |
| | 6 | 1 (QUGDUT) | 2.888 | | | | |
| | 7 | 1 (OCOXUA) | 2.896 | | | | |
| | 8 | 1 (DIQLUM) | 3.067 | | | | |

compounds with coordination numbers of 2 to 6 were observed with CN = 4 being the most dominant (20 hits) and CN = 6 being the least (with only one entry as at the time of preparing this manuscript). The mean Li-Im distance ranged from 2.111 to 2.191 Å, a difference of 0.08 Å with standard deviations ranging from 0.008 to 0.073. According to Hering et al. [27], increasing bulkiness of substituents on the N-positions of the Im ligand enforces minor elongations of the M-Im bond. Considering the large spectrum of N-substituted Im ligands used in the syntheses of these compounds, the observed standard deviations show that the high charge-to-size-ratio of the small $Li^+$ cation is the dominant factor in determining the strength of the Li-Im bond distance and not steric interactions by substituents on the Im ligand. Assessment of the mean Im-M-X angles shows that four-coordinate Li-Im compounds usually adopt tetrahedral geometries with mean bond angles of 111.8° (109.5° for an ideal tetrahedral configuration). The slight deviation could be attributed to steric interactions in the surrounding ligands. Jacobsen et al. [7] used the term "percent buried volume (%$V_{Bur}$)" to represent the fraction of the volume of a sphere centered on the metal, buried by overlap with atoms of the various NHC ligands. The bulkier the substituents on the NHC, the larger the %$V_{Bur}$. This molecular descriptor is analogous to Tolman's cone angle used to describe steric interactions in tertiary phosphines [28]. The wide spread (standard deviations of 12.45 to 19.31) of the reported bond angles could be attributed to the differences in the types of substituent on the imidazol-2-ylidene ring as well as the different types of auxiliary ligand with different %$V_{Bur}$ present in the complexes.

As shown in Figure 1, the overall distribution of the Li-Im bond ranges from 2.075 Å for three-coordinate compound to a maximum of 2.338 Å for four-coordinate compounds with 2.16 Å and 0.067 being the respective mean and standard deviation.

Sodium imidazol-2-ylidenes were the least of the group IA M-Im compounds, with 14 entries in the CSD. The dominant geometry (7 hits) is tetrahedral with average bond angles of 119.2°. Relative to Li-Im entries, the average bond length of the Na-Im is longer, with values ranging from 2.44 Å for two-coordinate complexes to 2.505 Å for four-coordinate species. This bond weakening effect can be attributed to the lower Lewis acidity of $Na^+$ relative to $Li^+$ [15]. Generally, the M-Im bond distances increased down the group with potassium imidazol-2-ylidenes recording average bond lengths in the range of 2.888 Å to 3.067 Å. Six entries were recorded for two-coordinate K-Im compounds with near-linear bond angles (mean of 178°). Despite the fact that $K^+$ is a weaker Lewis acid, the contact between $K^+$ and the carbene carbon has been described to be primarily electrostatic with negligible backbonding interactions [29]. Higher coordination numbers of six and seven were also recorded for $K^+$ probably due to its larger surface area.

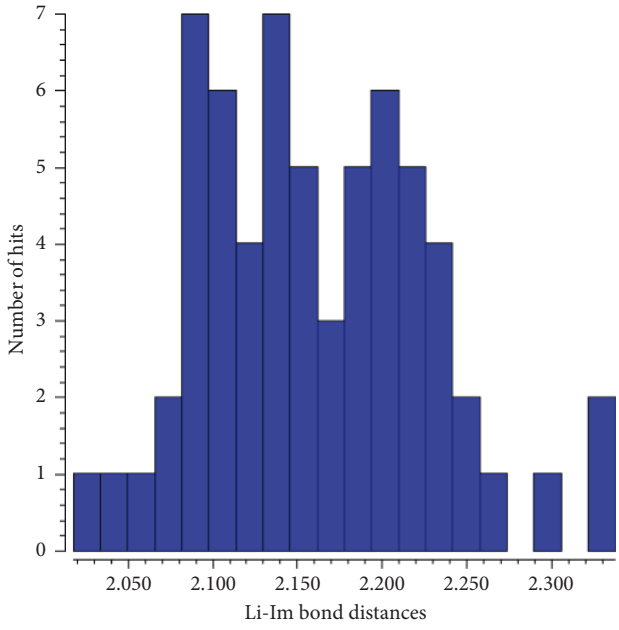


Figure 1: Distribution of the Li-Im bond lengths in the CSD.

As shown in Table 2, there are fewer entries of group IIA metal-imidazol-2-ylidenes in the CSD with Mg-Im

complexes being numerous (19 entries). These complexes are widely used as mild reducing agents [30]. Beryllium chemistry is relatively isolated because of the high toxicity of beryllium compounds [31]. Nonetheless, twelve crystal structures of beryllium imidazol-2-ylidenes were retrieved from the CSD. The observed Be-Im contacts are above the sum of the corresponding covalent radii [15]. The general preference for four-coordinate geometry of the group IA complexes is however different for the group IIA analogues. Coordination number of three is the dominant geometry for Be, whereas Mg and Ca recorded coordination numbers of four and six, respectively.

The increase in average bond length down group IIA corresponds to an overall increase in ionic size down the same group. The three-coordinate Be complexes have trigonal planar geometries with mean bond angles of 119.8°. The four-coordinate Mg-Im complexes are however tetrahedral (109.9°). The average bond angle of 96.6° recorded for the six-coordinate predominantly octahedral Ca-Im complexes is as a result of the fact that Im and any of the ancillary ligands are both axial and/or equatorial to each other. In such instances, the bond angles are nearly 90° or in few cases, the Im is trans to the ancillary ligand and the bond angles become nearly 180°. Generally, the average M-Im bond distances of the group IIA metal-imidazol-2-ylidenes are relatively shorter than their group IA analogues confirming the fact that the bonding mode between main-group metals and NHCs can be explained by the Lewis acid-base theory [13] as well as the electrostatic model [15]. This shows that group IIA metals are more electrostatic than the corresponding group IA analogues. The similarities between the mean M-Im bond distances of the Li-Im/Mg-Im and the Na-Im/Ca-Im pair can be attributed to diagonal relationships existing between these species. These relationships have been well documented and used to explain, for example, why $Li^+$ competes with $Mg^{2+}$ for metal-binding sites and subsequent inhibition of key enzymes in specific neurotransmission pathways [32].

From Table 3, it is clear that the Lewis acidity and the electrostatic potential are the dominant factors controlling the strength of the M-Im bonds. The strong Lewis acidity of the group IIIA element compounds can be attributed to the vacancy in their p-orbitals resulting from the incomplete octet. These vacancies are usually filled by dative covalent bonding with $\sigma$-donating ligands such as amines, phosphines, and carbenes [13].

The $\sigma$-donor ability of imidazol-2-ylidenes plays a pivotal role in the stabilization of these complexes. As shown in Table 3, the number of entries of the tetrahedrally coordinated complexes is in the order B-Im > Al-Im > Ga-Im. Boron, like lithium, also shows preference for Im complexes with coordination numbers ranging from 2 to 6 with tetrahedral geometries being the most dominant (101 entries). The number of group 3 tetrahedral M-Im complexes is about 50.6% of the total number of entries. Interests in these highly stabilized imidazol-2-ylidenes are growing because of their various applications as reagents and catalysts in organic synthesis [33]. Generally, the bond lengths decrease in the order Li-Im > Be-Im > B-Im, Na-Im > Mg-Im > Al-Im, and K-Im > Ca-Im > Ga-Im for the respective groups.

Figure 2 shows the distribution of B-Im distances in the respective tetrahedral complexes retrieved from the CSD. The bond lengths range from 1.515 Å to 1.71 Å with a standard deviation of 0.037. These B-Im bonds are the strongest (with mean bond lengths of 1.619 Å) of the M-Im bonds used for this study.

NHC-boranes have been identified as a new class of compounds which are readily accessible and stable such that they are treated as organic compounds rather than coordination complexes [33]. These tetravalent neutral complexes have a rich chemistry of their own and are poised to have an impact beyond main-group boron chemistry in both organic and radical polymerization chemistry [33]. The second part of this work therefore investigates the B-$C_{carbene}$ bond computationally using density functional theory (DFT) methods.

Different analogues of the parent ($i$Pr$_2$Im) $BH_3$ were optimized to investigate the effect of electron donating and electron withdrawing groups on the strength of the C1-B28 bond. As shown in Figure 3, seven analogues were chosen for this study.

The difference in the C1-B28 bond length between the gas phase optimized structure and that of the experimental structure (ALAZUJ in Table 4) was found to be 0.009 Å. The slight difference in the other bond parameters could be attributed to inter- and intramolecular interactions present in the solid-phase crystal structures which are absent in the gas phase optimized structures [34].

Generally, the presence of electron donating (OH) and electron withdrawing (F) substituents at the 2 and 3 positions of the imidazol-2-ylidene ring has negligible effects on the C1-B28 bond length as given by complexes **6** and **7**. Significant bond weakening was however observed in complexes **2**, **3**, **4,** and **5** when the substituents are on boron. The longest bond distance of 1.737 Å was recorded in **3** with $NH_2$ groups on boron. According to Vitaly et al. [13], there is a delicate balance between the steric and electronic effects in the borenium cation such that the $NH_2$ groups on boron can sterically interact with the isopropyl substituents on the N-positions of the imidazol-2-ylidene ligand to increase the length of the C1-B28 bond. Similar weakening of the boron-carbene bond was reported by Braunschweig et al. [35] who synthesized and characterized a series of carbene-stabilized boranes bearing sterically bulky diphenyldiselenides with isopropyl substituents on the N-atoms of the imidazol-2-ylidene ligand. This steric interaction has the tendency of increasing C16-N27-C1 [27]. As shown in Table 4, the C16-N27-C1 bond angle increased by 4.6° on going from **1** to **3**. Similarly, this bond angle is relatively unaffected when the substituents are on the 2 and 3 positions of the imidazol-2-ylidene ring as given in **6** and **7**.

The C1-B28 bond in the tetrahedral boranes was further studied by natural bond orbital (NBO) analysis at the DFT/B3LYP level of theory. NBO analysis provides the most accurate possible picture for describing chemical bonding that corresponds to the elementary Lewis dot diagram. It takes into consideration electronegativity of the participating atoms as well as their hybridizations. This gives an in-

Table 2: The number of entries (hits), coordination number (CN), and bond parameters of group IIA metal-imidazol-2-ylidenes.

| Metal | CN | No. of hits | D (M-Im) (Å) | | | Im-M-X angle (°) | |
|---|---|---|---|---|---|---|---|
| | | | Mean | Range | St dev. | Mean | St dev. |
| Be | 3 | 9 | 1.798 | 1.768–1.82 | 0.018 | 119.8 | 6.26 |
| | 4 | 2 | 1.811 | 1.8–1.822 | 0.016 | 108.9 | 4.99 |
| | 5 | 1 (MEHQIB) | 1.765 | | | | |
| Mg | 3 | 8 | 2.25 | 2.204–2.288 | 0.025 | 115.5 | 5.17 |
| | 4 | 9 | 2.226 | 2.194–2.285 | 0.032 | 109.9 | 7.96 |
| | 5 | 2 | 2.246 | 2.226–2.279 | 0.029 | 107.6 | 6.68 |
| Ca | 3 | 2 | 2.613 | 2.598–2.628 | 0.021 | 117.5 | 1.98 |
| | 5 | 2 | 2.547 | 2.509–2.582 | 0.027 | 104.9 | 30.3 |
| | 6 | 8 | 2.606 | 2.518–2.705 | 0.058 | 96.6 | 25.32 |
| | 7 | 2 | 2.619 | 2.562–2.702 | 0.045 | 100.2 | 31.86 |

Table 3: M-Im distances, bond angles, and coordination numbers (CN) of the group IIIA metal-imidazol-2-ylidenes.

| Metal | CN | No. of hits | D (M-Im) (Å) | | | Im-M-X angle (°) | |
|---|---|---|---|---|---|---|---|
| | | | Mean | Range | St dev | Mean | St dev |
| B | 2 | 1 (RUBSOY) | 1.484 | | | | |
| | 3 | 71 | 1.582 | 1.514–1.647 | 0.024 | 117.7 | 5.98 |
| | 4 | 101 | 1.619 | 1.515–1.71 | 0.037 | 111.2 | 5.86 |
| | 5 | 12 | 1.619 | 1.562–1.641 | 0.022 | 108.5 | 22.51 |
| | 6 | 1 (ZITFOY) | 1.558 | | | | |
| Al | 3 | 2 | 2.023 | 1.987–2.072 | 0.044 | 118.7 | 8.00 |
| | 4 | 63 | 2.063 | 1.964–2.163 | 0.034 | 107.8 | 5.73 |
| | 5 | 3 | 2.095 | 2.07–2.13 | 0.025 | 107.8 | 28.74 |
| | 6 | 2 | 2.185 | 2.17–2.198 | 0.010 | 104.9 | 33.97 |
| Ga | 2 | 2 | 2.240 | 2.189–2.288 | 0.055 | 111.3 | 9.70 |
| | 4 | 54 | 2.059 | 1.984–2.196 | 0.052 | 108.5 | 6.77 |
| | 5 | 1 (LEKBUA) | 1.978 | | | | |

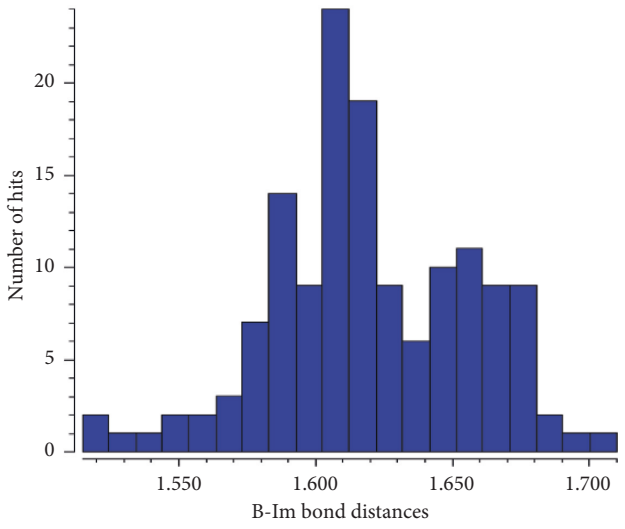


Figure 2: Distribution of B-Im bond lengths in tetrahedral boron imidazol-2-ylidenes.

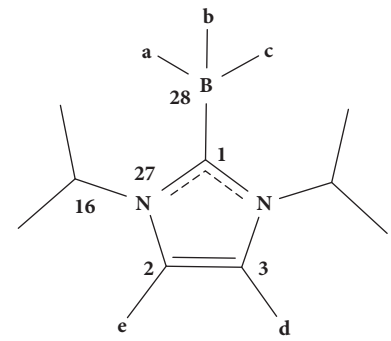


**1**, a = b = c = d = e = H;
**2**, a = b = c = OH, d = e = H;
**3**, a = b = c = $NH_2$, d = e = H;
**4**, a = b = c = CN, d = e = H;
**5**, a = b = c = F, d = e = H;
**6**, a = b = c = H, d = e = OH;
**7**, a = b = c = H, d = e = F;

Figure 3: Structures and numbering scheme of the imidazol-2-ylidene stabilized boranes.

depth understanding of the mode of bonding interaction between two or more atoms in a chemical structure. Table 5 gives the electron distributions in the C1-B28 bond of the optimized structures. In all the structures, the boron center is $sp^3$ hybridized with percent s-character ranging from 20.43 in **3** to 26.93 in **5**. However, the carbene carbon is predominantly sp hybridized with percent s-character ranging from 42.48 in **5** to 48.94 in **7**. This sp-hybridization suggests a partial double bond character [14] spanning the N-C-N substructure as shown in Figure 4.

Table 4: Selected bond lengths (Å) and bond angles (°) of the optimized borane complexes with the experimental reference in parenthesis.

| | 1 (ALAZUJ) | 2 | 3 | 4 | 5 | 6 | 7 |
|---|---|---|---|---|---|---|---|
| Bond length | | | | | | | |
| C1-B28 | 1.611 (1.602) | 1.712 | 1.737 | 1.657 | 1.675 | 1.612 | 1.610 |
| C1-N27 | 1.366 (1.362) | 1.363 | 1.374 | 1.366 | 1.361 | 1.366 | 1.369 |
| C16-N27 | 1.489 (1.474) | 1.500 | 1.503 | 1.512 | 1.500 | 1.489 | 1.495 |
| Bond angle | | | | | | | |
| N27-C1-B28 | 127.6 (129.5) | 127.5 | 127.6 | 127.1 | 127.2 | 127.3 | 127.3 |
| C16-N27-C1 | 128.4 (126.1) | 131.2 | 133.0 | 133.4 | 130.3 | 128.4 | 129.0 |

Table 5: Percent distribution of electrons in the C1-B28 bond with the corresponding s and p characters.

| Molecule | Electron density (*e*) | Percent C1 | Percent B28 |
|---|---|---|---|
| 1 | 1.966 | 67.95 (48.64%s : 51.36% p) | 32.05 (22.56%s : 77.35%p) |
| 2 | 1.956 | 72.44 (44.50%s : 55.50%p) | 27.56 (23.68%s : 76.19%p) |
| 3 | 1.949 | 72.14 (46.72%s : 53.28%p) | 27.86 (20.43%s : 79.45%p) |
| 4 | 1.944 | 64.78 (44.58%s : 55.14%p) | 35.22 (24.31%s : 75.64%p) |
| 5 | 1.970 | 72.24 (42.48%s : 57.51%p) | 27.76 (26.93%s : 72.92%p) |
| 6 | 1.969 | 67.90 (48.64%s : 51.36%p) | 32.10 (22.49%s : 77.43%p) |
| 7 | 1.967 | 68.15 (48.94%s : 51.06%p) | 31.85 (22.29%s : 77.36%p) |

The percent contribution of C1 and B28 to the shared pair of electrons shows that the C1-B28 bond is largely ionic/dative covalent with the carbene carbon contributing between 64.78% and 72.44% to the shared pair of electrons, thereby decreasing the electron density on C1. As shown in Table 6, the general atomic charge density on C1 in the isolated imidazole fragment is +0.094 *e*. This increased significantly to values between +0.249 *e* in complex **5** and + 0.411 *e* in complex **7**. Similarly, the electron density on B28 increased from slight positive charges to values as high as −0.462 *e* in **6** and −0.463 *e* in **7**.

The electron pull from C1 to B28 was also felt in N27. This conjugative effect is shown as a slight decrease in electron density on N27 in the complex as compared to its values in the isolated fragments. The natural charge on B28 also varied with the type of substituent. The highly electronegative atoms (such as fluorine) directly attached to the less electronegative boron center made it more positive with a charge density of +1.152 *e* in **5** as compared to the parent borane **1** where it is −0.441 *e*. Thus, the electrophilicity of the borenium atom can be fine-tuned by varying the type of substituents to give fragments for different applications [13].

The binding energy of the optimized complexes was also estimated at the DFT/B3LYP level of theory with polarization and diffuse functions added to minimize the basis set superposition error (BSSE). As each fragment uses the basis set of the others in the complex, smaller basis sets will result in decreased energy and an overestimation of the binding energy [36]. Generally, the interaction between the imidazol-2-ylidenes and the substituted boranes is made up of two factors: dative covalent bonding with $\sigma$-electron donation from the carbene carbon into $sp^3$ hybridized boron orbitals as well as intramolecular interactions between substituents on the borenium atom and the isopropyl groups on the N-atoms of the imidazol-2-ylidene ligand. The BSSE of all the complexes was corrected by the method of counterpoise correction introduced by Boys and Bernardi [37]. A similar method was used by Kirmse [38] to study the binding energies in carbene complexes of nonmetals. The counterpoise corrected binding energy ($\Delta E_{BE}^{CP}$) is the difference between the corrected total energy of the optimized complex ($E_{Complex}^{CP}$) and that of the constituent fragments ($E_1$ and $E_2$).

$$\Delta E_{BE}^{CP} = E_{Complex}^{CP} - (E_1 + E_2). \quad (1)$$

From equation (1), the more negative the calculated binding energy, the more stable the complex. As shown in Table 6, $\Delta E_{BE}^{CP}$ is strongest in **4** with a value of −227.2 kJ/mol followed by the parent borane **1** with −201.3 kJ/mol.

Complex **3**, with $NH_2$ substituents on the borenium ion was the least stable with a binding energy of +100.6 kJ/mol. Generally, substituents on the 2 and 3 positions of the imidazol-2-ylidene ligand have negligible effects on the C1-B28 bond as confirmed by the binding energies of **6** and **7** relative to the parent compound **1**. The relatively weak binding energies of **2** and **3** could be attributed to intramolecular steric interactions [7] between the OH groups on the borenium atom in **2** and the corresponding isopropyl substituents on the Im ligand as well as between the $NH_2$ groups and the iPr groups in **3**.

With regards to observations made in Tables 5 and 6 on the distribution of electrons and the accompanying charges on C1 and B28, the electrostatic potential surface of the complexes was plotted as shown in Figure 4.

The color scheme indicates that the boron atom becomes more electropositive when electronegative groups such as OH, $NH_2$, CN, and F are attached, as shown in complexes **2**, **3**, **4**, and **5**. The electron distribution in the C1-B28 bond is largely unaffected when these electron withdrawing groups

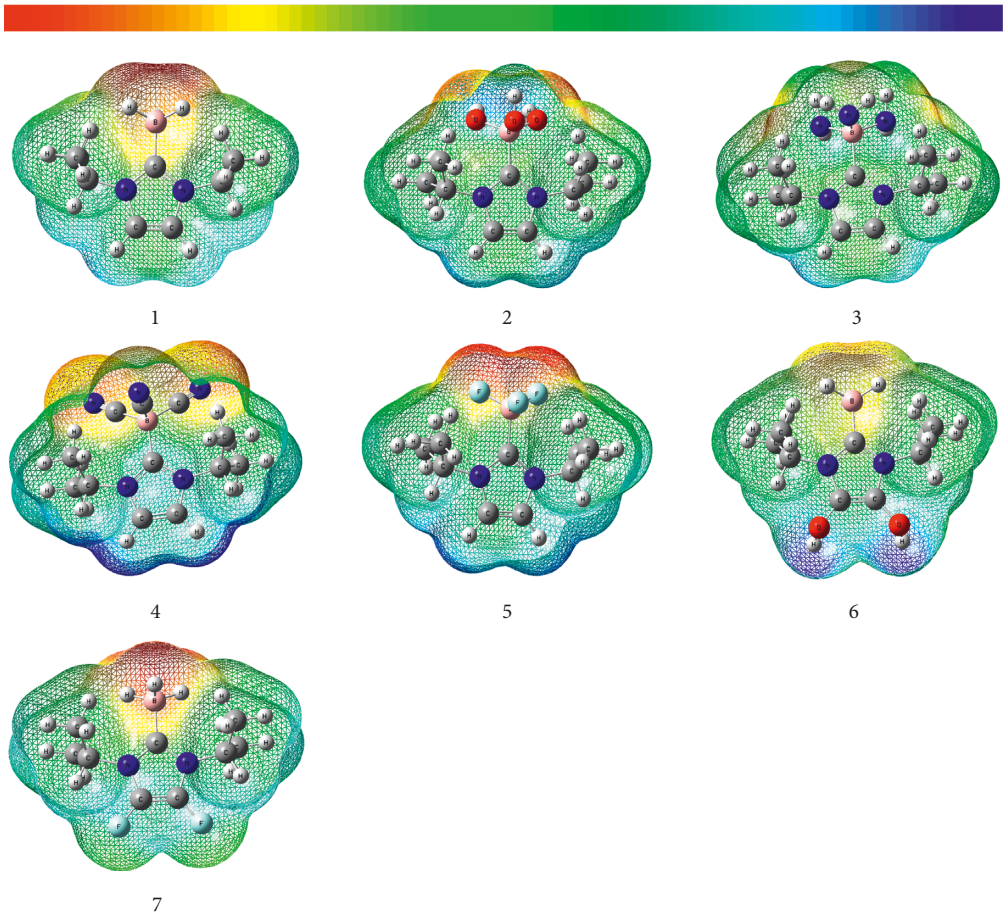


Figure 4: Electrostatic potential surface plot of the complexes at an isovalue of 0.001 a.u. Color ranges from red, more electronegative, through yellow to blue, more electropositive surface.

Table 6: Natural charge ($e$) of some selected atoms in the complex and isolated structures in addition to the BSSE corrected binding energies ($\Delta E_{BE}^{CP}$) of the complexes.

| Molecule | Atomic charge ($e$) | | | | | | Binding energy (kJ/mol) |
|---|---|---|---|---|---|---|---|
| | C1 | | B28 | | N27 | | |
| | Complex | Isolated | Complex | Isolated | Complex | Isolated | |
| **1** | +0.400 | +0.094 | −0.441 | +0.335 | −0.417 | −0.463 | −201.3 |
| **2** | +0.301 | +0.094 | +1.019 | +1.230 | −0.396 | −0.463 | −30.4 |
| **3** | +0.331 | +0.094 | +0.793 | +0.955 | −0.405 | −0.463 | +100.6 |
| **4** | +0.359 | +0.094 | −0.083 | +0.485 | −0.378 | −0.463 | −227.2 |
| **5** | +0.249 | +0.094 | +1.152 | +1.409 | −0.385 | −0.463 | −134.6 |
| **6** | +0.406 | +0.927 | −0.462 | +0.335 | −0.432 | −0.474 | −195.9 |
| **7** | +0.411 | +0.102 | −0.463 | +0.335 | −0.440 | −0.324 | −189.8 |

are bonded to the 2 and 3 positions of the imidazole ligand as observed in structures **6** and **7** relative to structure **1**.

## 4. Conclusion

This work used the relatively large number of group IA, group IIA, and group IIIA imidazol-2-ylidene complexes in the Cambridge Structural Database (CSD) to investigate their M-$C_{carbene}$ bond distances as well as the preferred geometries and coordination numbers. Generally, group IIIA metal-imidazol-2-ylidenes were the most abundant with 313 entries followed by group IA with 73 and group IIA with 45 entries. The average M-$C_{carbene}$ bond lengths were found to increase down each group and be similar along each diagonal. Potassium complexes presented the most diverse forms of coordination numbers ranging from CN = 2 to CN = 8. It was also observed that most of the metals except calcium formed complexes in which the metal ion is tetrahedrally coordinated. Dominant factors such as Lewis acidity and electrostatic attractions were found to control the bonding modes of the respective ions.

In all, tetrahedrally coordinated boron imidazol-2-ylidene complexes were the most numerous (101 entries). Natural bond orbital (NBO) analysis of these complexes bearing N-substituted isopropyl groups with various electron withdrawing and electron donating groups showed that the strength of the B-$C_{carbene}$ bond depends on the bulkiness of the substituents on the borenium atom which sterically interfere with the isopropyl groups on the N-atoms of the imidazol-2-ylidene ligand. This observation was further confirmed by estimation of the binding energy, natural charge, and the electron distribution in the B-$C_{carbene}$ bond.

## Data Availability

The data used to support the findings of this study are available from the corresponding author upon request.

## Conflicts of Interest

The author declares that there are no conflicts of interest regarding the preparation and publication of this paper.

## Acknowledgments

The author is grateful to the FAIRE program of the Cambridge Crystallographic Data Centre (CCDC) for the opportunity to use the Cambridge Structural Database (CSD) for the substructure searches, molecular visualization, and statistical analysis.

## References

[1] J. R. Miecznikowski and R. H. Crabtree, "Hydrogen transfer reduction of aldehydes with alkali-metal carbonates and iridium NHC complexes," *Organometallics*, vol. 23, no. 4, pp. 629–631, 2004.

[2] F. Wang, L.-j. Liu, W. Wang, S. Li, and M. Shi, "Chiral NHC–metal-based asymmetric catalysis," *Coordination Chemistry Reviews*, vol. 256, no. 9-10, pp. 804–853, 2012.

[3] L.-A. Schaper, S. J. Hock, W. A. Herrmann, and F. E. Kühn, "Synthesis and application of water-soluble NHC transition-metal complexes," *Angewandte Chemie International Edition*, vol. 52, no. 1, pp. 270–289, 2013.

[4] K. Öfele, W. A. Herrmann, D. Mihalios et al., "Mehrfachbindungen zwischen hauptgruppenelementen und übergangsmetallen: CXXVI. Heterocyclen-carbene als phosphananaloge liganden in metallkomplexen," *Journal of Organometallic Chemistry*, vol. 459, no. 1-2, pp. 177–184, 1993.

[5] W. A. Herrmann, "N-heterocyclic carbenes: a new concept in organometallic catalysis," *Angewandte Chemie International Edition*, vol. 41, no. 8, pp. 1290–1309, 2002.

[6] A. A. Tukov, A. T. Normand, and M. S. Nechaev, "N-heterocyclic carbenes bearing two, one and no nitrogen atoms at the ylidene carbon: insight from theoretical calculations," *Dalton Transactions*, no. 35, pp. 7015–7028, 2009.

[7] H. Jacobsen, A. Correa, A. Poater, C. Costabile, and L. Cavallo, "Understanding the M (NHC) (NHC = N-heterocyclic carbene) bond," *Coordination Chemistry Reviews*, vol. 253, no. 5-6, pp. 687–703, 2009.

[8] S. Gruendemann, A. Kovacevic, M. Albrecht, J. W. Faller, and R. H. Crabtree, "Abnormal ligand binding and reversible ring hydrogenation in the reaction of imidazolium salts with IrH5 (PPh3) 2," *Journal of the American Chemical Society*, vol. 124, no. 35, pp. 10473–10481, 2002.

[9] H. van Rensburg, R. P. Tooze, D. F. Foster, and A. M. Z. Slawin, "The synthesis and X-ray structure of the first cobalt Carbonyl–NHC dimer. Implications for the use of NHCs in hydroformylation catalysis," *Inorganic Chemistry*, vol. 43, no. 8, pp. 2468–2470, 2004.

[10] W. Gil, K. Boczoń, A. M. Trzeciak et al., "Supported N-heterocyclic carbene rhodium complexes as highly selective hydroformylation catalysts," *Journal of Molecular Catalysis A: Chemical*, vol. 309, no. 1-2, pp. 131–136, 2009.

[11] M.-L. Teyssot, A.-S. Jarrousse, M. Manin et al., "Metal-NHC complexes: a survey of anti-cancer properties," *Dalton Transactions*, no. 35, pp. 6894–6902, 2009.

[12] S. Tetteh, D. K. Dodoo, R. Appiah-Opong, and I. Tuffour, "Cytotoxicity, antioxidant and glutathione S-transferase inhibitory activity of palladium(II) chloride complexes bearing nucleobase ligands," *Transition Metal Chemistry*, vol. 39, no. 6, pp. 667–674, 2014.

[13] V. Nesterov, D. Reiter, P. Bag et al., "NHCs in main group chemistry," *Chemical Reviews*, vol. 118, no. 19, pp. 9678–9842, 2018.

[14] E. Baba, T. R. Cundari, and I. Firkin, "N-heterocyclic carbenes of the late transition metals: a computational and structural database study," *Inorganica Chimica Acta*, vol. 358, no. 10, pp. 2867–2875, 2005.

[15] S. Bellemin-Laponnaz and S. Dagorne, "Group 1 and 2 and early transition metal complexes bearing N-heterocyclic carbene ligands: coordination chemistry, reactivity, and applications," *Chemical Reviews*, vol. 114, no. 18, pp. 8747–8774, 2014.

[16] P. Pyykkö and M. Atsumi, "Molecular single-bond covalent radii for elements 1–118," *Chemistry—A European Journal*, vol. 15, no. 1, pp. 186–197, 2009.

[17] G. Kuppuraj, M. Dudev, and C. Lim, "Factors governing Metal–Ligand distances and coordination geometries of metal complexes," *The Journal of Physical Chemistry B*, vol. 113, no. 9, pp. 2952–2960, 2009.

[18] Lr. Ruĺišek and J. Vondrášek, "Coordination geometries of selected transition metal ions (Co2+, Ni2+, Cu2+, Zn2+, Cd2+, and Hg2+) in metalloproteins," *Journal of Inorganic Biochemistry*, vol. 71, no. 3-4, pp. 115–127, 1998.

[19] S. Tetteh, "Coordination behavior of Ni2+, Cu2+, and Zn2+ in tetrahedral 1-methylimidazole complexes: a DFT/CSD study," *Bioinorganic Chemistry and Applications*, vol. 2018, Article ID 3157969, 8 pages, 2018.

[20] I. J. Bruno, J. C. Cole, P. R. Edgington et al., "New software for searching the Cambridge Structural Database and visualizing crystal structures," *Acta Crystallographica Section B Structural Science*, vol. 58, no. 3, pp. 389–397, 2002.

[21] C. F. Macrae, P. R. Edgington, P. McCabe et al., "Mercury: visualization and analysis of crystal structures," *Journal of Applied Crystallography*, vol. 39, no. 3, pp. 453–457, 2006.

[22] M. Frisch, G. Trucks, H. Schlegel et al., *Gaussian 09, Revision A. 1 [computer Software]*, Gaussian Inc., Wallingford, CT, USA, 2009.

[23] A. Frisch, A. Nielson, and A. Holder, *User Manual GaussView*, Gaussian Inc., Pittsburgh, PA, USA, 2000.

[24] A. D. Becke, "Density-functional exchange-energy approximation with correct asymptotic behavior," *Physical Review A*, vol. 38, no. 6, pp. 3098–3100, 1988.

[25] S. Tetteh, A. Quashie, M. A. Anang, and A. Quashie, "Purification, characterization, and time-dependent adsorption

studies of Ghanaian muscovite clay," *Journal of Chemistry*, vol. 2018, Article ID 4193657, 8 pages, 2018.

[26] M. Dudev, J. Wang, T. Dudev, and C. Lim, "Factors governing the metal coordination number in metal complexes from Cambridge Structural Database analyses," *The Journal of Physical Chemistry B*, vol. 110, no. 4, pp. 1889–1895, 2006.

[27] F. Hering, J. H. J. Berthel, K. Lubitz et al., "Synthesis and thermal properties of novel NHC-stabilized cobalt carbonyl nitrosyl complexes," *Organometallics*, vol. 35, no. 17, pp. 2806–2821, 2016.

[28] C. A. Tolman, "Steric effects of phosphorus ligands in organometallic chemistry and homogeneous catalysis," *Chemical Reviews*, vol. 77, no. 3, pp. 313–348, 1977.

[29] M. S. Hill, G. Kociok-Köhn, and D. J. MacDougall, "N-Heterocyclic carbenes and charge separation in heterometallic s-block silylamides," *Inorganic Chemistry*, vol. 50, no. 11, pp. 5234–5241, 2011.

[30] S. P. Green, C. Jones, and A. Stasch, "Stable magnesium (I) compounds with Mg-Mg bonds," *Science*, vol. 318, no. 5857, pp. 1754–1757, 2007.

[31] P. Boffetta, J. P. Fryzek, and J. S. Mandel, "Occupational exposure to beryllium and cancer risk: a review of the epidemiologic evidence," *Critical Reviews in Toxicology*, vol. 42, no. 2, pp. 107–118, 2012.

[32] T. Dudev and C. Lim, "Competition between Li+and Mg2+in metalloproteins. Implications for lithium therapy," *Journal of the American Chemical Society*, vol. 133, no. 24, pp. 9506–9515, 2011.

[33] D. P. Curran, A. Solovyev, M. Makhlouf Brahmi, L. Fensterbank, M. Malacria, and E. Lacôte, "Synthesis and reactions of N-heterocyclic carbene boranes," *Angewandte Chemie International Edition*, vol. 50, no. 44, pp. 10294–10317, 2011.

[34] M. Hanus, M. Kabeláč, J. Rejnek, F. Ryjáček, and P. Hobza, "Correlated ab initio study of nucleic acid bases and their tautomers in the gas phase, in a microhydrated environment, and in aqueous solution. Part 3. Adenine," *The Journal of Physical Chemistry B*, vol. 108, no. 6, pp. 2087–2097, 2004.

[35] H. Braunschweig, I. Krummenacher, C. Lichtenberg et al., "Dibora[2]ferrocenophane: a carbene-stabilized diborene in a strainedcis-configuration," *Angewandte Chemie International Edition*, vol. 56, no. 3, pp. 889–892, 2017.

[36] M. D. Esrafili, "Characteristics and nature of the intermolecular interactions in boron-bonded complexes with carbene as electron donor: an ab initio, SAPT and QTAIM study," *Journal of Molecular Modeling*, vol. 18, no. 5, pp. 2003–2011, 2012.

[37] S. F. Boys and F. Bernardi, "The calculation of small molecule interactions by the difference of separate total energies. Some procedures with reduced errors," *Molecular Physics*, vol. 19, no. 4, pp. 553–566, 1970.

[38] W. Kirmse, "Carbene complexes of nonmetals," *European Journal of Organic Chemistry*, vol. 2005, no. 2, pp. 237–260, 2005.